MULTI-TEMPORAL SATELLITE ANALYSIS OF MORPHODYNAMIC CHANGE IN THE PERANCAK SANDSPIT, BALI, INDONESIA

***Adzkia Noerma ARIFA*[1,*], *Bayu MUNANDAR*[2,3] *& Amir Yarkhasy YULIARDI*[4]**

DOI: 10.21163/GT_2026.213.08

ABSTRACT

Perancak Sandspit, located in Jembrana Regency, is one of the coastal landforms on the southwest coast of Bali, Indonesia. It is a large hook-shaped sandspit that experienced morphodynamic change between January 2024 and January 2025. The results reveal three periods of sandspit shortening and one period of sandspit elongation. During the first period, January to March 2024, and the third period, July to September 2024, the sandspit experienced shortening at a rate of about 0.3 meters/day. The second period, April to June 2024, was the only period of sandspit elongation with a rate of 0.59 meters/day. Although the sandspit elongated, its width remained unchanged from the first period at 150 meters. Conversely, in the fourth period, October 2024 to January 2025, the sandspit shrank significantly at a rate of 1.16 meters/day, with a concurrent decrease in width. In addition, in the first and fourth periods, changes in the direction of the distal end of the Perancak sandspit were observed, which were pushed toward the east-northeast. The result indicates that the longshore sediment transport rate during the elongation phase is around 104,000 m^3/year. Although the Perancak sandspit exhibits fluctuations in morphology and geometry, its overall characteristics in January 2025 remained similar to those observed in January 2024. It indicates recurring morphological and geometric variations of the Perancak sandspit.

Keywords: *Sandspit; Morphodynamic change; Multi-temporal; Longshore sediment transport rate; Bali.*

1. INTRODUCTION

Sandspit is one of the coastal landforms in the form of narrow and elongated sediment deposits. It is dominantly formed by longshore currents. The proximal part of the sandspit was always connected to the mainland, and the distal part often curves following the dominant wave direction. Sandspits were found on irregular shorelines where sediment availability and wave energy allowed the smoothing of the coastline by maintaining the direction of longshore currents and moving toward the coastal re-entrants or bay (Orford, 2006).

Morphological and geometrical changes of sandspits were best observed in a plan view perspective. Many studies have examined the dynamics of sandspits through field observations, analytical solutions, numerical and physical modeling, as well as satellite imagery analysis (Duy et al., 2023). Among these methods, satellite imagery analysis was the most widely used (Lawson et al., 2021).

[1] *Department of Marine Science, Faculty of Fisheries and Marine Science, Universitas Diponegoro, Indonesia. *Corresponding author: adzkia@lecturer.undip.ac.id (ANA).*

[2] *Department of Oceanography, Faculty of Fisheries and Marine Science, Universitas Diponegoro, Indonesia, bymunandar@gmail.com (BM).*

[3] *Study Program of Fisheries and Marine Technology and Business, Faculty of Fisheries and Marine Science, Universitas Diponegoro, Indonesia.*

[4] *Department of Marine Science, Faculty of Fisheries and Marine Science, Universitas Jendral Soedirman, Indonesia, amiryarkhasy@gmail.com (AYY).*

The length and width of a sandspit were the functions of the availability of sediments and net longshore-directed wave-generated transport. In general, the dominant sediment found in its deposits was fine sediments such as sand, but gravel-dominated spits could also be found if the main component of the sediment availability on the coast was also dominated by gravel. On the other hand, mud-dominated sandspits were unlikely to form because the spits were formed by the breaking wave activity (Orford, 2006).

Moreover, the formation of a sandspit on the coast generated a backspit lee with low-energy currents, such as tides and small waves, and the deposition of fine sediments in the form of tidal banks and salt marshes. The morphological and geometrical changes of sandspits would affect the river flow patterns and the sedimentation systems at the estuary. These conditions have impacted the coastal ecosystems and fishermen's navigation access, the coastal land use, and escalated the flood risk in the downstream areas.

Bali, Indonesia, including the Jembrana Regency, has shown a diversity of coastal dynamics due to the natural and anthropogenic processes. The Perancak Village is located on the southwest coast of Bali and directly borders the Bali Strait (**Fig 1**). The Bali Strait is a narrow passage that lies between Java and Bali, linking the Java Sea on the northern side and the Indian Ocean on the southern side. The bathymetry of the Bali Strait is characterized by a shallow area in the middle section, but becomes steeper in the southern part and is exposed directly to the Indian Ocean (Berlianty and Yanagi, 2015).

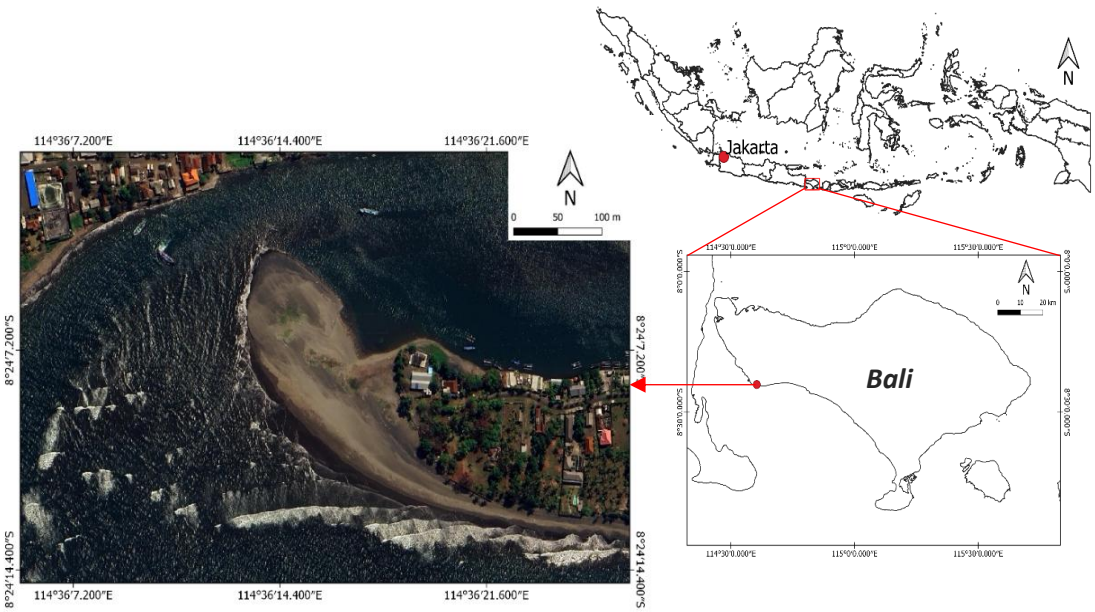

Fig. 1. Location of Bali in Indonesia (**right**) and the Perancak sandspit on the southwest coast of Bali (**left**).

The majority of its people worked as fishermen and farmers. The area also features other attractions, including turtle conservation sites and mangrove forests. In Perancak Village, a sandspit over 100 meters wide extends at the mouth of the Perancak estuary. As well as the Perancak beach, which consisted of medium sand on the bottom sediment (Paluphi et al., 2020), the Perancak sandspit was also constructed by fine sediment, such as sand. The anchoring area for fishing boats and the main tourist spot are located on the backspit.

Although multi-temporal satellite imagery analysis has been widely applied in coastal studies, its integration with sediment transport quantification to investigate the sandspit dynamics remains limited, particularly in the Perancak area. Due to the numerous strategic activities in the area, the sandspit dynamics here will affect local community livelihoods and existing tourism activities. Therefore, this study focuses on the morphological and geometrical changes of the sandspit found in Perancak, Jembrana, Bali, Indonesia.

2. MATERIALS AND METHODS

2.1. Satellite Image Analysis and Geometric Characteristics

The methodology employed in our study is depicted in **Fig 2**. The approach used in our study was satellite imagery analysis for the period of January 2024 to January 2025. First, the Sentinel-2 images were collected to observe the morphological and geometrical changes of the Perancak sandspit. These images were obtained from the Copernicus Data Space Ecosystem (**Table 1**). Second, the water line was distinguished from the sand using the modified normalized difference water index (MNDWI) at a resolution of 20 meters.

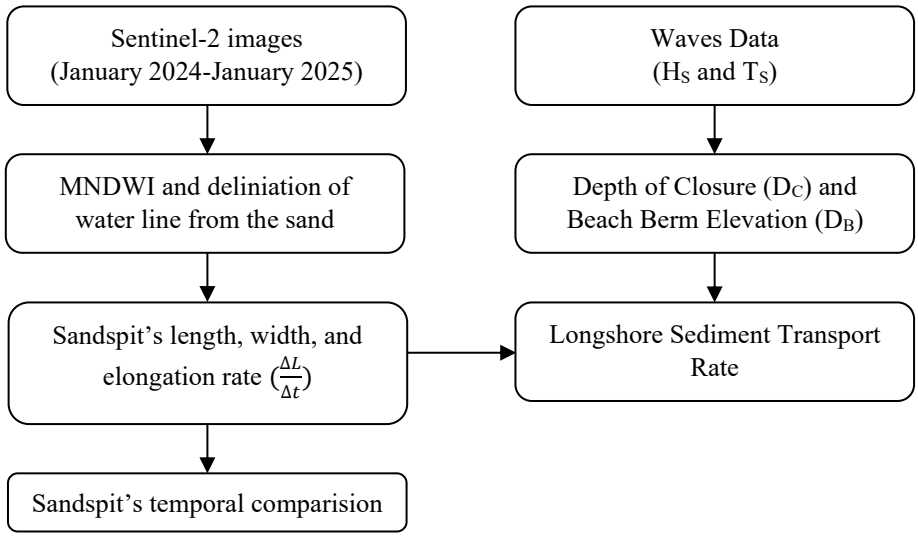

Fig. 2. Flow diagram for the research procedure.

Table 1.

An overview of Sentinel-2 data used in this study.

Date (dd/mm/yyyy)	Sensor	Resolution	Data Source
30/01/2024	Multispectral Instrument	10 m and 20 m	Sentinel-2
29/02/2024			
30/03/2024			
29/04/2024			
29/05/2024			
28/06/2024			
23/07/2024			
22/08/2024			
21/09/2024			
26/10/2024			
20/11/2024			
14/01/2025			

MNDWI was adopted because it was more suitable to improve the water information and can extract the water bodies more accurately than NDWI (Xu, 2006 and Du et al., 2016). The MNDWI from Sentinel-2 images was obtained through raster calculation using the following formula:

$$MNDWI = \frac{X_{green} - X_{SWIR}}{X_{green} + X_{SWIR}} \quad (1)$$

where X_{green} is the green band or Band 3 and X_{SWIR} is the short-wave infrared band or Band 11 of Sentinel-2.

Third, the length (L) and width (W) components were calculated based on the sandspit geometry. The length (L) component was drawn from the proximal point to the distal point of the sandspit. Meanwhile, the width (W) component was drawn transversely from the spit-platform geometry at the hook section.

2.2. Wave Data, Depth of Closure, and Beach Berm Elevation

The data used in this study include the wave data in the area of the Bali Strait (**Fig 3**), emphasizing the temporal change of the sandspit. The wave reanalysis data are from WAVERYS product (https://data.marine.copernicus.eu/product/GLOBAL_MULTIYEAR_WAV_001_032). The wave data were used for the calculation of the depth of closure (D_C) and the beam elevation (D_B). The depth of closure (D_C) and the beam elevation (D_B) were calculated using empirical calculations.

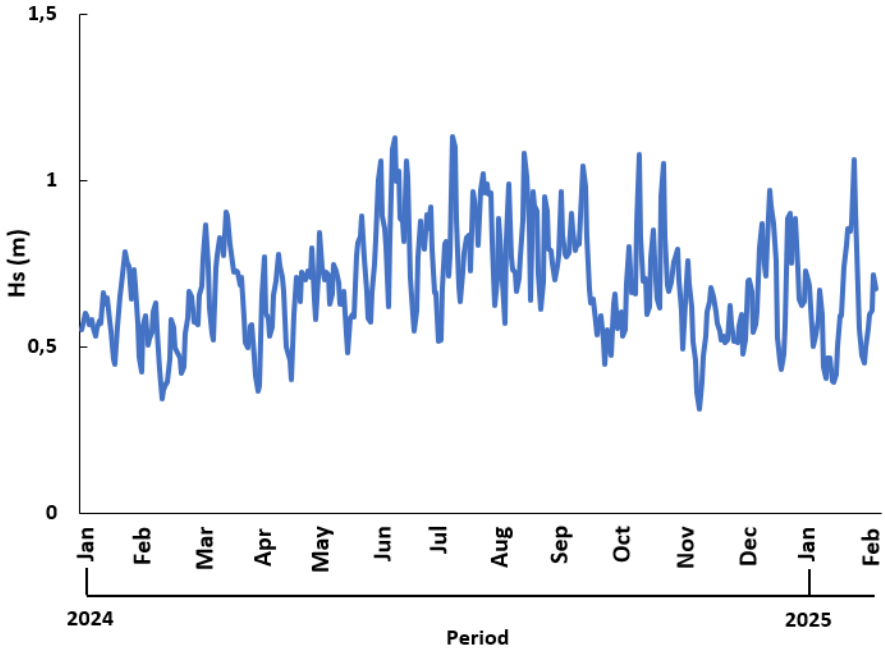

Fig. 3. The significant wave height between January 2024 and January 2025.

Two crucial factors for estimating the longshore sediment transport rate are the depth of closure (D_C) and the beam elevation (D_B). The depth of closure refers to the maximum offshore depth at which cross-shore sediment transport is negligible under normal wave and tide conditions (Durkin, Seenath & Knaapen, 2025). The depth of closure (D_C) was calculated using the equation proposed by Hallermeier (1978,1981) as follows:

$$D_C = 2.28H_{se} - 68.5\left(\frac{H_{se}^2}{gT_{se}^2}\right) \quad (2)$$

where Hse and Tse are the significant wave height and wave period of the extreme wave condition that is expected 12 h per year (Hallermeier, 1978) and g is the acceleration caused by gravity.

Hallermeier defined another equation of depth of closure based on the relationship between *Hse* and the annual mean of significant wave height as:

$$D_C = 2\bar{H}_s + 11\sigma_s \quad (3)$$

where σ_S is the standard deviation of the significant wave height.

In addition, the beach berm is a natural form of beach profile created by onshore sediment transport due to waves in the swash zone (Zhu et al., 2022). The beam elevation is the vertical distance from the crest of the berm to the specific datum, usually the mean sea level. An empirical equation relating the depth of closure to the berm elevation was defined by Uda (1997, as cited in Lawson et al., 2021 and Duy et al., 2023) and is represented as follows:

$$D_B = 0.32 \times D_C \quad (4)$$

2.3. Longshore Sediment Transport Estimation Model and Sandspit Growth Rate

The longshore sediment transport rate (LSTR) was estimated in this study using a straightforward mathematical calculation based on the methodology of Lawson et al. (2021). A schematic diagram of the model is shown below:

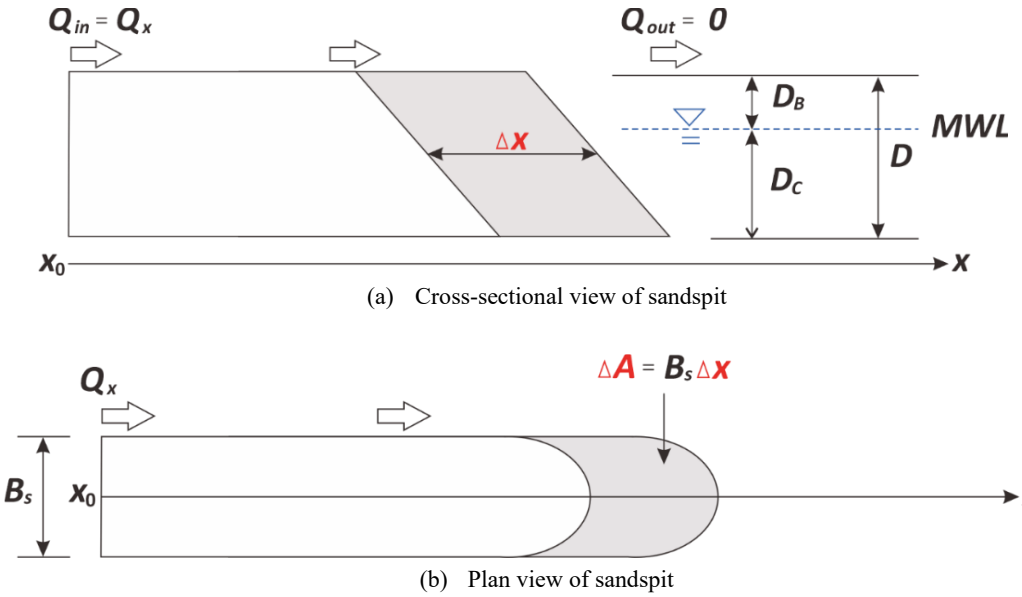

Fig. 4. Redrawn from Lawson et al. (2021), this schematic representation of the sandspit development process shows (a) a cross-sectional view and (b) a plan view.

According to the Lawson et al. (2021) model, the gradient in longshore sediment transport $Q_{in} = Q_x$ is thought to contribute to the sandspit's elongation directly, while the sandspit's width (B_S) remains constant throughout its growth and there is no sediment loss at its tip ($Q_{out} = 0$). The assumption of $Q_{out} = 0$ is used to obtain the first-order approximation of longshore sediment transport by simplifying the sediment budget and neglecting sediment losses at the tip. Moreover, the depth of closure (D_C) plus the berm elevation (D_B) adds up to the depth of active sediment (D). Given the above assumption, the LSTR can be calculated as follows:

$$Q_{in} = \bar{Q}_x = D \times \frac{\Delta A}{\Delta t} \tag{5}$$

where D is the depth of active sediment motion, calculated as $D_C + D_B$, and $\Delta A/\Delta t$ represents the sandspit area changes over a given time period. $\Delta A/\Delta t$ can be substituted by:

$$\frac{\Delta A}{\Delta t} = B_S \times \frac{\Delta L}{\Delta t} \tag{6}$$

where B_S refers to the width of the sandspit, which is considered constant over the elongation period, and $\Delta L/\Delta t$ is the elongation rate of the sandspit, which was determined from the image analysis.

Thus, the LSTR can be determined as:

$$Q_{in} = Q_x = (D_B + D_C) \times B_S \times \frac{\Delta L}{\Delta t} \tag{7}$$

Studies by Udo, Ranasinghe & Takeda (2020), and Razak & Khan (2020) have addressed the constraints of using Equation (2). By contrasting the outcomes of field surveys of wave conditions with wave data obtained from the models, these limitations were found. The cumulative error of our estimations reflects the ±20% error tolerance we imposed on our depth of closure calculations due to these limitations.

The temporal variation of the length change ($\Delta L/\Delta t$) and width change ($\Delta B_S/\Delta t$) were calculated using linear regression. Furthermore, we used a straightforward mathematical formula proposed by Duc Anh et al. (2020a) to predict the rate of sandspit growth in the elongation period as a function of the LSTR and sandspit width.

The hypothesis assumes that the sandspit width will remain constant during the elongation phase. The LSTR calculation in this study follows a similar assumption. This assumption leads to the following expression for the sandspit growth rate as follows:

$$R_S = \frac{Q_x}{(D_C + D_B)} \times \frac{1}{B_S} \tag{8}$$

where Q_x is the LSTR, D_C is the depth of closure, D_B is the berm elevation, and B_S is the sandspit width.

3. RESULTS AND DISCUSSION

3.1. Temporal Variation of Sandspit Geometry

3.1.1 Sandspit Length

Sandspits are attached to the land at one end and are longer than they are wide (Huggett, 2007). Based on research by Weidman and Ebert (1993), morphological changes in sandspits occurred cyclically and the periodic systems improved our understanding of inlet genesis and beach-barrier or sandspit evolution. Therefore, analyzing the temporal shoreline changes of the Perancak sandspit is important to understand the morphological dynamics. Changes in the shoreline of the Perancak sandspit are shown in **Fig 5**. It was shown that there were several periods of shortening and elongation from January 2024 to January 2025. Furthermore, we divided the morphological and geometrical timeframes into four periods (**Fig 6**). In this case, the elongation and shortening events were used to distinguish the periods.

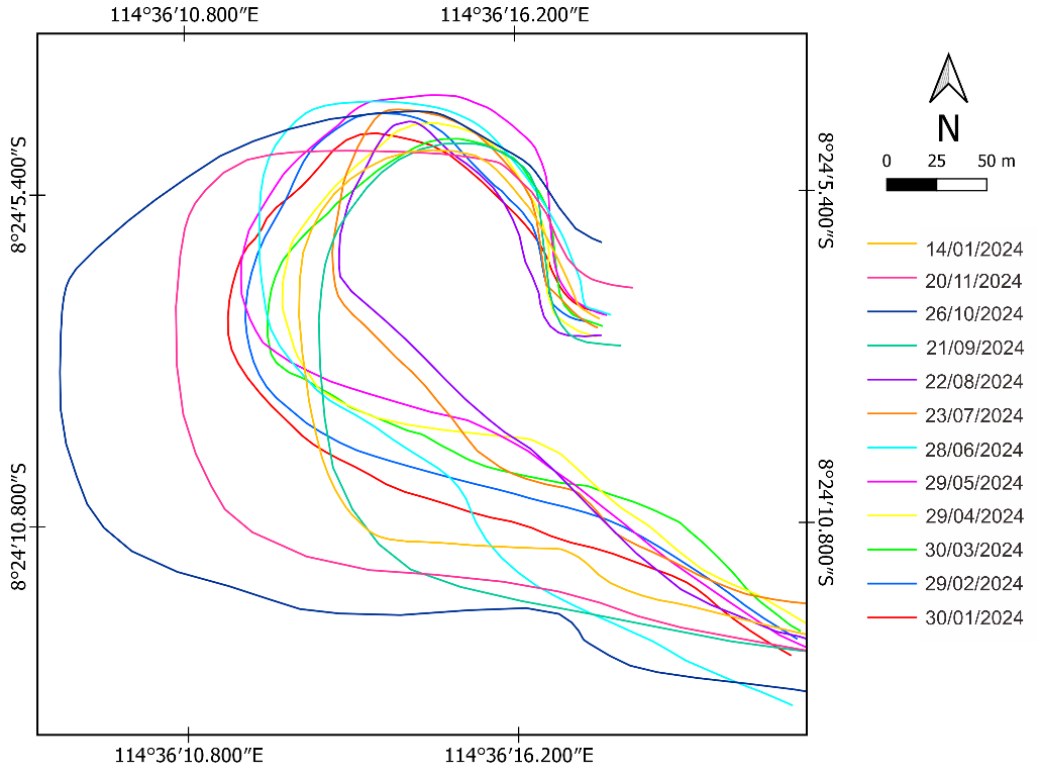

Fig. 5. Temporal variation of the Perancak sandspit's shoreline.

In the first period, January to March 2024, the sandspit experienced a gradual reduction in length or shortening. The rate of reduction was 0.33 meters/day. During the second period, April to June 2024, the sandspit experienced elongation and uninterrupted growth. The growth rate of the Perancak sandspit in this period was 0.59 m/day. Meanwhile, afterwards, a shortening was observed in July, indicating the end of Perancak sandspit growth in the second period.

In the third period, July to September 2024, a gradual reduction in the length occurred, similarly to the first period, with a rate of 0.36 meters/day. This period ended with significant sandspit growth until October 2024, with an increase of about 105.57 meters. This growth rate was 3.11 meters/day. In the fourth period, October 2024 to January 2025, a significant reduction in the length of the Perancak sandspit occurred with a rate of 1.16 meters/day.

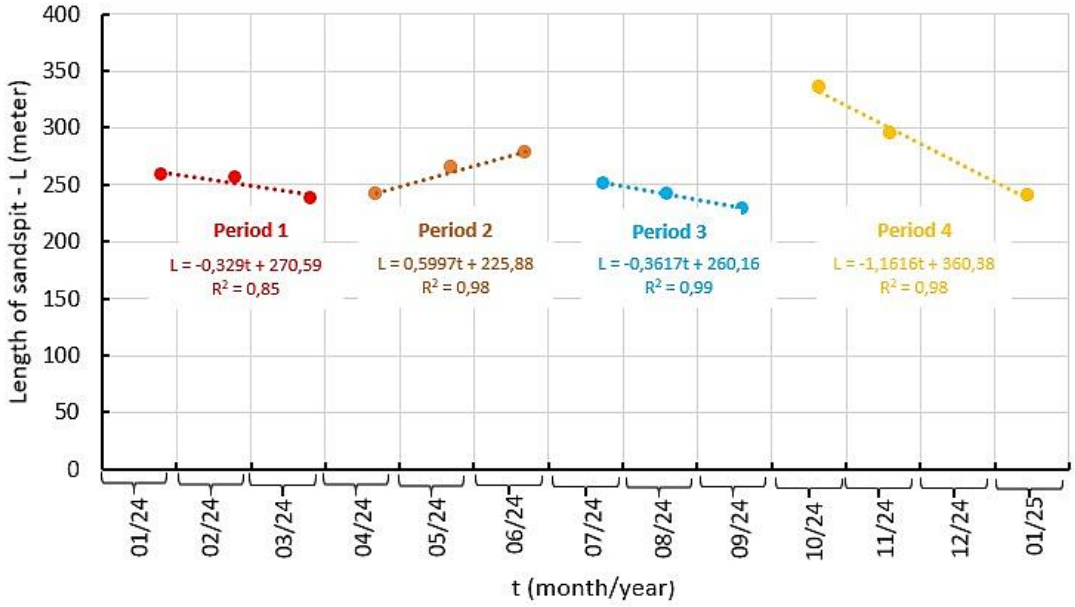

Fig. 6. Elongation and shortening of the Perancak sandspit from January 2024 to January 2025.

The sandspit dynamics are strongly linked to the sediment budget on the coast and/or the wave energy (Escudero et al., 2019). These factors play an important role in controlling the balance between erosion and sediment deposition along both the distal end and the body of the sandspit. When wave energy increases, erosion and sediment redistribution tend to dominate, causing shortening and morphological changes. In contrast, when sediment supply and depositional processes are dominant, the sandspit experiences elongation.

We indicated that the shortening during the first and the third periods was caused by gradual erosion at the distal tip. Hence, the erosional processes exceeded the sediment supply during these periods. In the first period, the wave energy increased compared to early January. The west monsoon, which is characterized by dominant winds from the west-northwest, generates higher-energy wave conditions. Furthermore, the shortening observed during the third period corresponded with the peak of the east monsoon, which also showed relatively higher wave conditions. These conditions likely intensified erosional processes at the distal end and enhanced sediment redistribution along the shoreline.

In contrast, the shortening was more notable and occurred at a higher rate during the fourth period. Compared to the first period, relatively higher wave energy prevailed during this period. We indicated this condition triggered rapid erosion at the spit-platform tip within a short period, whereas the sediment supply may have remained insufficient to compensate for ongoing erosion at the distal end. Moreover, the elongation occurred in the second period during the transitional phase toward the east monsoon. Wave conditions during this period were relatively favorable for sediment deposition, allowing sediment supply to accumulate at the distal end of the sandspit.

Besides the changes in the sandspit's length, the changes in the distal end of the Perancak sandspit were observed. In general, the Perancak sandspit is oriented northwest with a large hooked sandspit type. In the first and fourth periods, the curvature at the distal end of the sandspit appeared to be pushed toward the east-northeast or landward migration. The direction change occurred because of the changes in the dominant direction and energy of prevailing waves originating from the west, which propagated into the estuary area, affecting and altering the Perancak spit-platform. The wave refraction and diffraction around the inlet mouth caused sediment transport pathways to shift landward and reorient the distal end curvature. In addition, the wave penetration into the estuary area

during high-energy conditions increased the reworking of the sediment at the distal end. This reinforces the confidence that the Perancak sandspit developed within a wave-dominated inlet system. Such sandspits were commonly associated with the accumulation of sediments at their tips, which was introduced by longshore transport (Taveneau et al., 2024).

3.1.2 Sandspit Width

Fig. 7 shows the temporal variation of the width of the Perancak sandspit. In the first to second periods, January to June 2024, the width of the sandspit did not exhibit a significant change, remaining around 150 meters. During the first period, the sandspit experienced gradual erosion at the distal tip while maintaining a constant width. This condition suggests that the sediment redistribution occurred along the longitudinal axis, with erosion mainly concentrated at the distal tip rather than distributed across the entire body. Moreover, during the second period, the sandspit experienced elongation while maintaining a constant width. This condition indicates that the sediment deposition mainly occurred at the distal tip of the spit rather than at the entire body.

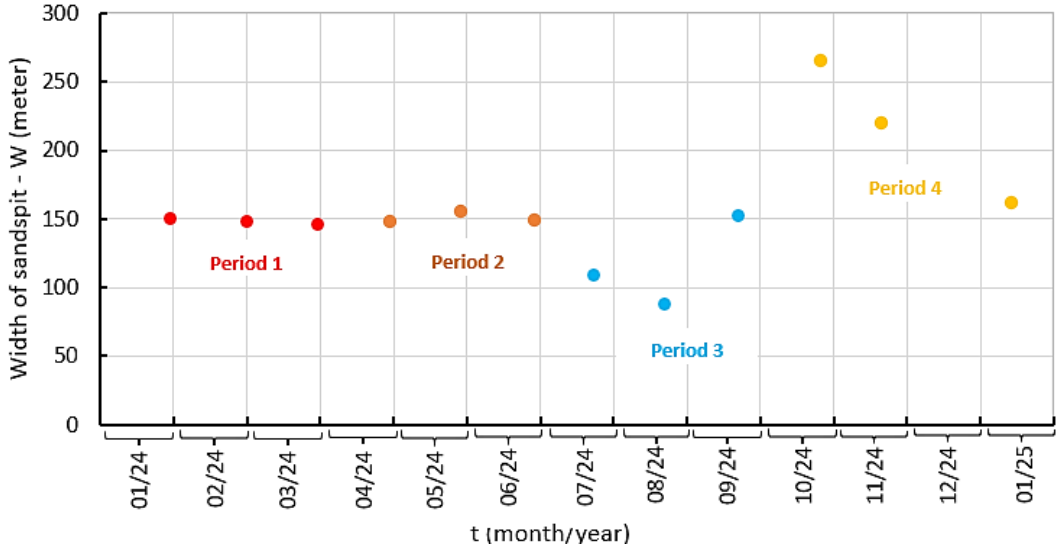

Fig. 7. Temporal variation of the Perancak sandspit's width from January 2024 to January 2025.

In the third period, July to September 2024, a larger change in the sandspit's width was observed and it did not occur uniformly throughout the entire period. From July to August 2024, the sandspit experienced a decrease in width. However, in September 2024, the curvature of the spit platform increased, and a significant widening was observed compared to the previous month. In August, the sandspit's width was only 87.26 meters, but it increased to 152 meters in September 2024. This widening continued to October 2024 with an additional increase of 112.19 meters.

Although shortening occurred in the third period, the morphological changes were not uniform. From July to August, both sandspit length and width decreased. This condition indicates that erosion occurred at both the distal end and lateral margins of the sandspit. However, in September 2024, the sandspit width increased despite the shortening trend, indicating that sediment redistribution temporarily shifted toward lateral deposition along the spit body.

A very distinct pattern was observed in October 2024, when the sandspit's length increased rapidly and the feature also widened. This condition is interpreted as a result of an increase in sediment budget accompanied by a reduction in wave energy. Subsequently, the sandspit's width decreased gradually during the fourth period, reaching 160.41 meters in January 2025. This reduction in width is likely due to the disruption of sediment supply and erosion of the sandspit tip. The width of the sandspit in that month did not differ considerably from that in January 2024.

3.2. Longshore Sediment Transport Rate and Sandspit Growth

As shown in **Fig. 6**, four distinct periods of the Perancak sandspit development were identified over one year. Based on the significant wave height and the wave period, the values of the beach berm elevation (D_B) and the depth of closure (D_C) were estimated at 0.78 m and 2.45 m, respectively. Therefore, the LSTR was calculated based on the elongation period derived from the image analysis. Using the elongation rate ($\Delta L/\Delta t$)) of the sandspit and Equation (7), the LSTR during the elongation period was estimated at 104,000 m^3/year. The results from this study indicate that the LSTR of the Perancak sandspit is in the order of 10^5 m^3/year with the LSTR estimations having an average error margin of $\pm 2.5 \times 10^4$ m^3/year.

Furthermore, the sandspit growth calculated using Equation (8) was estimated at 214 m/year, showing good agreement with the value derived from the satellite image analysis (215 m/year). This agreement suggests that the applied approach reasonably represents the morphological development of the Perancak sandspit. Nevertheless, the estimated LSTR may slightly overestimated due to the assumptions applied, particularly the assumption of negligible sediment losses at the tip.

Additionally, this study compares the characteristics of the Perancak sandspit with other sandspits worldwide, which were analyzed using similar approach, including the Badreveln in Sweden and the Fire Island in USA assessed by Hoan et al. (2011), the Sangomar in Senegal assessed by Palalane et al. (2014), Volta River in Ghana and Bouche du Roi in Benin studied by Lawson et al. (2021), as well as several sandspits in Vietnam, including the Loc An examined by Duc Anh et al. (2018), the Cua Loa examined by Duy et al. (2018), the Ly Hoa and the An Du examined by Duc Anh et al. (2020a), the Ken and the Phan examined by Duc Anh et al. (2020b), and the Song Tranh examined by Duy et al. (2023) (**Fig 8**, **Table 2**).

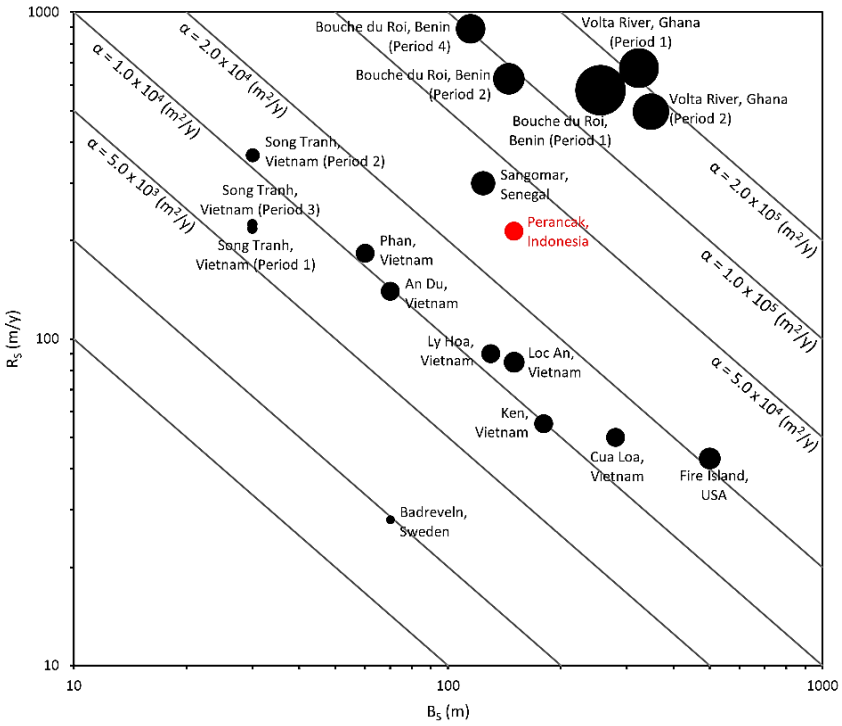

Fig. 8. Comparison of the sandspit growth rate and the sandspit width of the Perancak sandspit with that of other sandspits.

Based on the comparative data, the position of Perancak sandspit indicates a moderate category compared to other sandspits. The Perancak sandspit is narrower than the Volta River sandspit and the Bouche du Roi sandspit, although its growth rate remains relatively high. It indicates that an active accretion process and sediment supply occur in the area. In addition, the condition suggests that the longshore sediment transport plays an important role in the sandspit dynamics. Compared with several sandspits in Vietnam, the Perancak sandspit shows a higher growth rate at a similar width. It implies that the Perancak sandspit dynamics are more active and change rapidly.

Table 2.
Summary of morphodynamic properties of Perancak sandspit and other sandspits worldwide.

Study Area	B_S (m)	R_S (m/y)	LSTR (m^3/y)
Indonesia			
Perancak	150	214	104,000
Vietnam			
Loc An	150	85	200,000
Cua Loa	280	50	160,000
Ly Hoa	130	90	130,000
An Du	70	140	170,000
Ken	180	55	133,000
Phan	60	183	145,000
Song Tranh (Period 1)	30	217	39,000
Song Tranh (Period 2)	30	365	66,000
Song Tranh (Period 3)	30	224	40,000
Sweden			
Badreveln	70	28	10,000
USA			
Fire Island	500	43	220,000
Benin			
Bouche du Roi (Period 1)	255	578	1,980,000
Bouche du Roi (Period 2)	145	626	781,000
Bouche du Roi (Period 4)	115	889	734,000
Senegal			
Sangomar	124	300	465,000
Ghana			
Volta River (Period 1)	324	674	1,290,000
Volta River (Period 2)	348	496	1,210,000

Furthermore, the high dynamics of the sandspit may affect the stability of the river mouth through the inlet migration and sedimentation around the Perancak estuary. The sandspit dynamic may significantly influence the coastal community, fisheries activities, and mangrove habitat in the area. Thus, continuous monitoring of the sandspit dynamics is important to support sustainable coastal management and to mitigate the impacts on the surrounding area.

4. CONCLUSIONS

The analysis of morphological and geometrical changes of the Perancak sandspit, conducted using satellite imagery analysis from January 2024 to January 2025, shows several variations. The main findings can be summarized.

Three periods of shortening or reduction in sandspit length and one period of sandspit growth were identified. In the first period, January to March 2024, and the third period, July to September 2024, the sandspit experienced gradual shortening. Conversely, in the second period, April to June 2024, an elongation and growth phase occurred, and the sandspit width remained around 150 meters. In the

fourth period, October 2024 to January 2025, both the length and width of the sandspit decreased, presumably due to reduced sediment supply and intensified erosion at the spit tip.

The orientation of the Perancak sandspit's hook shifted toward the east–northeast during this period, driven by changes in wave energy and strengthened waves and winds from the west–southwest impacting the sandspit.

Image analysis and empirical calculation based on a one-line model were used to estimate the LSTR along the sandspit in the elongation period. The result was 104,000 m^3/year.

Although the sandspit underwent considerable temporal variability within the year, the geometry of the Perancak sandspit in January 2025 did not differ from its condition in January 2024. This suggests that seasonal variation is the dominant factor controlling sediment supply, wave conditions, and longshore currents around Perancak Beach, thereby influencing the temporal variability of the Perancak sandspit geometry.

ACKNOWLEDGEMENT

This research was funded by the non-APBN DPA LPPM 2025, Universitas Diponegoro, under Contract No: 222-150/UN7 D2/PP/IV/2025, with Addendum No: 745/UN7.D2/PP/X/2025.

REFERENCES

Berlianty, D. & Yanagi, T. (2015) Tide and tidal current in the Bali Strait, Indonesia. *Marine Research in Indonesia*. 36 (2), 25–36. doi:10.14203/mri.v36i2.39.

Du, Y., Zhang, Y., Ling, F., Wang, Q., Li, W. & Li, X. (2016) Water bodies' mapping from Sentinel-2 imagery with modified normalized difference water index at 10-m spatial resolution produced by sharpening the SWIR band. *Remote Sensing*. 8 (4). doi:10.3390/rs8040354.

Duc Anh, N.Q., Duy, D. Van & Viet, N.T. (2018) Elongation of sand spit at Loc An river mouth, Southern Vietnam. *Journal of Japan Society of Civil Engineers Ser B3 (Ocean Engineering)*. 74.

Duc Anh, N.Q., Tanaka, H., Tam, H.S., Tinh, N.X., Tung, T.T. & Viet, N.T. (2020a) Comprehensive study of the sand spit evolution at tidal inlets in the central coast of Vietnam. *Journal of Marine Science and Engineering*. 8 (9). doi:10.3390/JMSE8090722.

Duc Anh, N.Q., Tanaka, H., Tinh, N.X. & Viet, N.T. (2020b) Sand spit morphological evolution at tidal inlets by using satellite images analysis: Two case studies in Vietnam. *Journal of Science and Technology in Civil Engineering (STCE) - NUCE*. 14 (2), 17–27. doi:10.31814/stce.nuce2020-14(2)-02.

Durkin, C.J., Seenath, A. & Knaapen, M.A.F. (2025) A critical review of closure depth theories and uncertainties: implications for shoreline modelling and coastal management. *Ocean and Coastal Management*. 267. doi:10.1016/j.ocecoaman.2025.107732.

Duy, D. Van, Tanaka, H., Mitobe, Y., Duc Anh, N.Q. & Viet, N.T. (2018) Sand spit elongation and sediment balance at Cua Lo inlet in Central Vietnam. *Journal of Coastal Research*. (81), 32–39.

Duy, D. Van, Ty, T. Van, Thanh, T.N., Minh, H.V.T., De, C. Van, Duong, V.H.T., Dan, T.C., Viet, N.T. & Tanaka, H. (2023) Sand spit morphology at an inlet on Phu Quoc Island, Vietnam. *Water (Switzerland)*. 15 (10). doi:10.3390/w15101941.

Escudero, M., Silva, R., Hesp, P.A. & Mendoza, E. (2019) Morphological evolution of the sandspit at Tortugueros Beach, Mexico. *Marine Geology*. 407, 16–31. doi:10.1016/j.margeo.2018.10.002.

Hallermeier, R.J. (1981) A profile zonation for seasonal sand beaches from wave climate. *Coastal Engineering*. 4 (4), 253–277.

Hallermeier, R.J. (1978) Uses for a calculated limit depth to beach erosion. In: *Coastal Eningeering, Proceedings of the 16th Conference on Coastal Engineering*. 1978 Hamburg, Germany, ASCE: Reston, VA, USA. pp. 1493–1512.

Hoan, L.X., Hanson, H., Larson, M. & Kato, S. (2011) A mathematical model of spit growth and barrier elongation: Application to Fire Island Inlet (USA) and Badreveln Spit (Sweden). *Estuarine, Coastal and Shelf Science*. 93 (4), 468–477. doi:10.1016/j.ecss.2011.05.033.

Huggett, R.J. (2007) *Fundamentals of Geomorphology*. 2nd edition. Routledge.

Lawson, S.K., Tanaka, H., Udo, K., Hiep, N.T. & Tinh, N.X. (2021) Morphodynamics and evolution of estuarine sandspits along the Bight of Benin Coast, West Africa. *Water*. 13 (21). doi:10.3390/w13212977.

Orford, J. (2006) Encyclopedia of Geomorphology. In: A.S. Goudie (ed.). *Encyclopedia of Geomorphology*. New York, Routledge, International Association of Geomorphologists. p.

Palalane, J., Larson, M. & Hanson, H. (2014) Analytical model of sand spit evolution. In: *34th International Conference on Coastal Engineering (ICCE 2014)*. January 2014 pp. 1187–1194.

Paluphi, W.R., Muskananfola, M.R. & Sugianto, D.N. (2020) Analysis of sediment dynamics in the waters Perancak and Pengambengan Beaches, Jembrana-Bali. *International Journal of Oceans and Oceanography*. 14 (2), 257–276.

Razak, M.Ab. & Khan, A.R. (2020) Development of a predictive closure depth equation using field data and wave refraction modelling. In: *IOP Conference Series: Materials Science and Engineering*. 29 May 2020 Institute of Physics Publishing. p. doi:10.1088/1757-899X/849/1/012093.

Taveneau, A., Almar, R. & Bergsma, E.W.J. (2024) On the cyclic behavior of wave-driven sandspits with implications for coastal zone management. *Estuarine, Coastal and Shelf Science*. 303. doi:10.1016/j.ecss.2024.108798.

Udo, K., Ranasinghe, R. & Takeda, Y. (2020) An assessment of measured and computed depth of closure around Japan. *Scientific Reports*. 10 (1). doi:10.1038/s41598-020-59718-5.

Xu, H. (2006) Modification of normalised difference water index (NDWI) to enhance open water features in remotely sensed imagery. *International Journal of Remote Sensing*. 27 (14), 3025–3033. doi:10.1080/01431160600589179.

Zhu, J., Shi, F., Cai, F., Wang, Q., Qi, H., Zhan, C., Liu, J., Liu, G. & Lei, G. (2022) Influences of beach berm height on beach response to storms: A numerical study. *Applied Ocean Research*. 121. doi:10.1016/j.apor.2022.103090.